


RESEARCH

Open Access



Response of Aswan cable-stayed bridge to spatial non-synchronous seismic excitations

Maryam A. Seleemah¹, Mohamed S. Helam², Mohamed A. Abu-alenein², Eslam B. Hammad²,
Mohamed S. Goda², Ayman A. Seleemah¹ and Amr Z. Elkady^{1*} 

*Correspondence:
amrzaki@f-eng.tanta.edu.eg

¹ Department of Structural
Engineering, Faculty
of Engineering, Tanta University,
Tanta, Egypt

² Assistant Researcher, Tanta,
Egypt

Abstract

Cable-stayed bridges are important infrastructure facilities serving the world today. Therefore, their safety against earthquake ground motions is crucial. However, due to their long spans, the affecting seismic excitations might be spatially non-synchronous. This paper presents a study of the effect of non-synchronous seismic excitations on Aswan cable-stayed bridge located at southern Egypt. Nonlinear time history analysis was conducted on a three-dimensional finite element model of the bridge. The spatial variability was represented in terms of the wave passage effect which was simulated via different delay times between the arrivals of the ground motion to bridge supports. Results indicated that spatial variability of earthquake ground motion has, in general, a favorable effect on most bridge response parameters. This is attributed to the flexibility of the overall bridge provided by the flexibility of the bridge structural system and/or by existence of seismic isolation.

Keywords: Aswan bridge, Multi-support excitation, Seismic behavior, Wave passage effect, Cable-stayed bridge

Introduction

Cable-stayed bridges are aesthetically appealing infrastructures that became popular over the past few decades. They are characterized by increased stiffness and timely efficient construction methods [1–4]. Many researchers aimed to study their behavior under Identical Support Excitation (ISE). For example, Clemente et al. [5] utilized a finite element model, based on the experimental static and seismic behavior of Indian cable-stayed bridge to evaluate the seismic load effect on the bridge. Hao et al. [6] studied the dynamic behavior of a typical cable-stayed bridge under lateral earthquake excitations. Elkady et al. [7] introduced a hybrid analytical–experimental technique to simulate the earthquake excitations on a cable-stayed bridge. The failure of one of the support anchorage plates of an existing steel cable-stayed bridge located at high seismic zone was studied by Javanmardi et al. [8]. Camara and Astiz [9] investigated the retrofit solutions of cable-stayed bridges with supplemental damping devices connecting the deck and the tower in the transverse direction. Zhang et al. [10] simulated steel truss cable-stayed bridge under different seismic accelerations in the case of a high-speed train traversing

the bridge during earthquake. Liu et al. [11] dissipated the earthquake energy by using viscous dampers in Hangzhou Bay cable-stayed bridge. Camara and Astiz [12] compared the static pushover procedures and nonlinear dynamic response history analysis to study the nonlinear seismic behavior of cable-stayed bridges. El Ouni et al. studied the numerical and experimental dynamic analysis and control as well as health monitoring of cable-stayed bridges [13].

These studies on cable-stayed bridges assumed that all the support motions are identical which is somehow unrealistic in these structures [14]. Typical cable-stayed bridges are generally characterized by their long spans. Due to such long spans, the seismic behavior of these structures is affected by the spatial variability in the ground motions [15]. Such variability occurs due to wave passage effect, incoherence effect and local soil effect [16]. Ignoring these effects would significantly overestimate or underestimate the seismic behavior of these bridges [17].

The effects of spatially changing ground motions on structures can be represented by Multi-Support Excitation (MSE) [18–23], multi-support response spectrum [24], and multi-support random vibration [25–27]. However, the nonlinearity of long-span structures would not be modeled in the response spectrum and random vibration techniques. Therefore, the MSE becomes a good alternative to model seismic responses under spatially varying earthquake excitations. Unfortunately, the recordings at nearby bridge sites to the earthquake ground motions are rare. To overcome this, researchers utilized theoretical techniques to simulate spatially varying seismic motions. For example, Somerville et al. [28], Vanmarcke and Fenton [29], Bi and Hao [30], Liao and Zerva [31], and Konakli and Kiureghian [32] studied spatially varying earthquake excitation based on the coherency function coupled with theoretical target power spectral density functions. Saxena et al. [33] considered the three causes of seismic variability to estimate the bridge structure response through non-linear time history analysis. They characterized the “wave passage effect” in terms of wave propagation apparent velocity, the “incoherence effect” by a coherence function, and the “local soil effect” by response spectra at different locations. Deodatis [34] generated the earthquake time histories acting at the bridge supports utilizing a variation of the spectral representation method. Sextos et al. [35] used the recorded spatially variable earthquake ground motions during two seismic events to model the response of Evripos bridge. The non-synchronous excitation of the bridge excited higher modes of vibration and suppressed the oscillation of its fundamental mode. Fontara et al. [36] studied the site effects, spatial variability of seismic motion, and soil-structure interaction on the inelastic response of bridge structures. Both synchronous and non-synchronous seismic effects on the bridge were determined. It was concluded that the positive or the negative effect of the spatially variable seismic motion depends on the interplay of all the key parameters of bridge. Recently, Ramadan et al. [37] investigated the effect of soil types, level of loss in coherency, and the difference in the arrival time of the seismic motions. Zhong et al. [38] utilized a set of 100 ground motions to conduct MSE analysis for the effect of spatial variability parameters on the fragility curves of cable-stayed bridges.

Some studies investigated the response of seismically isolated cable-stayed bridges [39, 40]. Other studies focused on the behavior of seismically isolated cable-stayed bridges under MSE. For instance, Patel et al. [41] studied the seismic response of cable-stayed

bridge isolated with Triple Friction Pendulum System (TFPS) under MSE. Base shear and acceleration were decreased whereas displacement was increased due to MSE. Masrilayanti et al. [42] found a significant discrepancy between the seismic analysis of an 800-m long cable-stayed bridge upon application of ISE and MSE. The ISE caused lower responses if the ground motion magnitudes were similar to the small magnitude of the multi-support excitation. Similarly, Alexander et al. [18] found that the ISE analysis of structural mode coupling was not conservative compared to MSE analysis in cable-stayed bridges

One of the important cable-stayed bridges in Egypt is the Aswan cable-stayed bridge located at the south of the country. This bridge, while considered a very important infrastructure, received very little research work. Abdel-Zaher et al. [40] conducted ambient vibration tests on the bridge to estimate its modal parameters. The test was performed using a 300-kN truck traffic load and used eleven positions to monitor the bridge response. Abou-Rayan [43] studied its static and dynamic characteristics utilizing finite-element method. The results revealed existence of strong coupling in all orthogonal directions within most vibration modes.

Up to the author's knowledge, no studies were performed to investigate the effect of seismic variability on the behavior of Aswan cable-stayed bridge. Thus, the current research represents an effort to get an insight into the effect of non-synchronous seismic excitations on the behavior of such important infrastructural facility. For this, five different earthquake records were utilized and based on the general types of soils located in Egypt, and the spatial variability was represented in terms of the wave passage effect. Therefore, different delay times between the arrivals of the ground motions to the bridge supports were considered. Nonlinear time history analysis was conducted on a three-dimensional finite element model of the bridge taking the geometric and material nonlinearities into consideration. Key response parameters were investigated. These include base shear at the bridge supports, pylon displacements, pylon shear forces, deck displacements, cable forces, and base isolator response.

Methods

Description of Aswan cable-stayed bridge

Located on the Nile River near Aswan city in Egypt, the Aswan cable-stayed bridge was built in 2002. The main bridge consists of a concrete deck, one-plane of cables and two towers (see Fig. 1). Figure 2 shows a general layout of the bridge along with typical cross-sections at selected locations.



Fig. 1 Aswan cable-stayed bridge (<https://structurae.net/en/structures/aswan-bridge>)

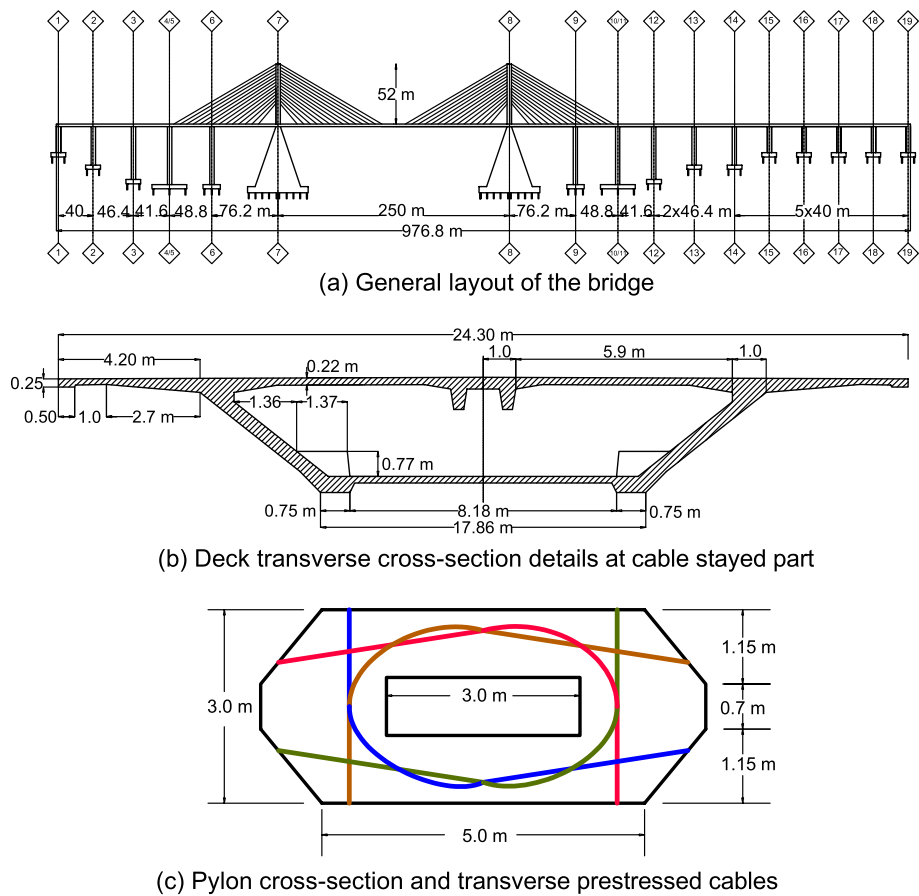


Fig. 2 General layout and typical cross sections of Aswan Cable-Stayed Bridge. **a** General layout of the bridge. **b** Deck transverse cross-section details at cable-stayed part. **c** Pylon cross-section and transverse prestressed cables

Table 1 Material properties of concrete and stay cables steel of the bridge

Material	Unit weight (kN/m ³)	Strength (MPa)	Modules of elasticity (GPa)	Poisson ratio
Concrete	23.2	45	30	0.2
Stay cable steel	78.6	1767	200	0.3

The bridge deck has a central main span of 250 m and two side spans of 125 m each with an overall length of 500 m [43]. It consists of prestressed concrete segments with trapezoidal box shape having two inclined 42-cm-thick webs. The box-girder has a height and width of 3.3 and 24.3 m, respectively. Tables 1, 2 and 3 summarize the material properties, properties of cables and general description of the bridge. Special arrangements were designed to prevent local buckling due to the large width of the box-girder and the force transmission from the cables to the deck. For example, the top slab was stiffened using two longitudinal girders at the middle part of the box-girder. Moreover, it was transversally prestressed via 4F15S tendons. Furthermore, the bottom slab was longitudinally stiffened by two rigid beams at the intersections

Table 2 Properties of the cables

Cable type	No. of strands	Area (m ²)	Weight per unit length (kN/m)	Allowable cable force (kN)	Ultimate cable force (kN)
Cable 1	109	0.0329	2.86	21664	28885
Cable 2	91	0.0246	2.14	18086	24115
Cable 3	73	0.0227	1.97	14509	19345

Table 3 General description of the bridge

Bridge total length	925 m	Main span length	250 m	Side span length	125 m
Bridge width	24.3 m	Deck typical span	40 m	Pylon height	52 m
Number of bearings on top of each main pier			16	Bearing size	1.0*1.0*0.16 m
Deck cross section type	Prestressed single box section with a trapezoidal shape				
Pylon cross section type	Prestressed irregular eight-polygon shape				
Type of bridge cables	One-plane semi-fan type of cables composed of 73 to 109 H15 strands surrounded by an HDPE tube				
Number of bridge cables	Totally 56 stay cables with 14 stay cables on each side of the pylon				

with the two inclined webs and transversely stiffened by a cross beam having a 30-cm depth. The hollow box main girder was designed to insure considerable torsional rigidity such that to keep the deformations due to eccentric live load on the bridge deck within allowable limits.

The bridge contains one vertical plane with 56 cables at its central longitudinal axis. The bridge cables are composed of 73 to 109 H15 strands incased in HDPE tubes. Each strand has diameter of 15.7 mm and contains 7 wires. The breaking load per strand is 265 kN. Strands are galvanized, waxed, and individually HDPE sheathed. The cables are anchored to the deck every two-deck segments (i.e., at 7.812 m spacing). The cables are attached to the tower in a semi-fan shape through a vertical height of 30 m.

The prestressing forces in the cables plays a crucial role in maintaining the allowable displacement and distribution of bending moments along the bridge deck [44, 45]. In Aswan bridge, five phases of tensioning the stay cables were implemented. These included three phases during the balanced cantilever construction. The fourth phase followed the placing of the superimposed dead loads and the final phase was carried out after 18 months of operation to reduce the effect of creep.

Looped post-tensioning tendons transfer of the stay forces to the towers. The bridge has two hollow box-shaped towers (pylons). Each tower consists of a transversally prestressed concrete hollow-box section and is fixed to the deck. Figure 2b shows a cross-section of the towers. The tower is 55 m high from the deck level. The main part of the bridge has six piers (axis 5 to 10 in Fig. 2a). The piers on axis 5, 6, 9, and 10 have reinforced concrete box sections. The main pier shaft located on axis 7 and 8 consists of a massive reinforced concrete block with pyramidal shape with dimension of 24×25 m at bottom. It is supported on a raft over 88 piles 1.1m diameter each, see Fig. 3. It is worth mentioning that the ground conditions at the east bank comprise medium dense sand overlying dense uniform sand. The geology at the west bank is

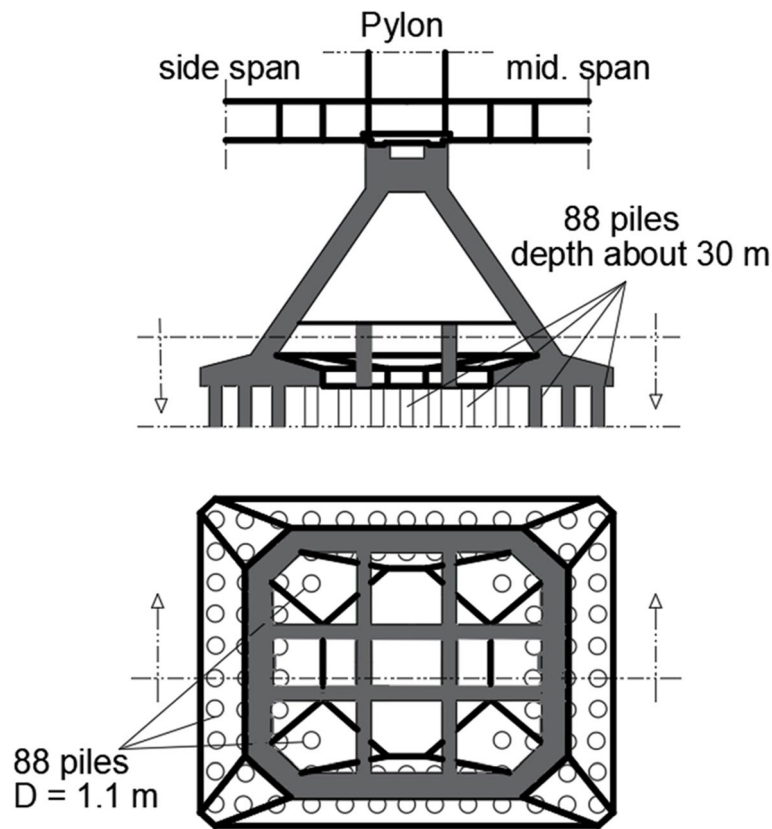


Fig. 3 General layout of piers on axis 7 and 8 and the pile arrangement

more variable however, consisting of sub-surface sand overlying silty sandstone. At deeper levels, a hard layer of shale with fragments of sandstone is encountered.

The bridge is seismically isolated just under the girder level. At the main piers on axis 7 and 8, two lines of isolators are placed on top of each pier. Each line has eight isolators to support the bridge deck. The size of the isolator is $1000 \times 1000 \times 160$ mm. Two PTFE, $600 \times 600 \times 60$ mm bearings are placed on piers 5, 6, 9, and 10 to allow for the longitudinal motions and to control the horizontal ones. For additional details on the bridge refer to [46, 47].

Equation of motion of bridge subjected to multiple seismic excitations

The general dynamic equation of motion of a bridge subjected to seismic excitation can be written as

$$M\ddot{\mathbf{U}} + C\dot{\mathbf{U}} + K\mathbf{U} = -M\Gamma\ddot{\mathbf{x}}_a \quad (1)$$

where \mathbf{U} , $\dot{\mathbf{U}}$, and $\ddot{\mathbf{U}}$ are the displacement, velocity, and acceleration response vectors, respectively; K , C , and M are the stiffness, damping, and mass matrices of the structure, respectively. $\ddot{\mathbf{x}}_a$ and Γ are the longitudinal ground acceleration and a vector which contains ones and zeros to relate the ground acceleration to the various degrees of freedom of the bridge. For the case of multi-support excitation however, the model can be modified to include the degrees of freedom of the supports. Hence, the dynamic equilibrium

equation for all the degrees of freedom of the bridge is presented in the following partitioned form.

$$\begin{bmatrix} M & M_g \\ M_g^T & M_{gg} \end{bmatrix} \begin{bmatrix} \ddot{U}^t \\ \ddot{U}_g \end{bmatrix} + \begin{bmatrix} C & C_g \\ C_g^T & C_{gg} \end{bmatrix} \begin{bmatrix} \dot{U}^t \\ \dot{U}_g \end{bmatrix} + \begin{bmatrix} K & K_g \\ K_g^T & K_{gg} \end{bmatrix} \begin{bmatrix} U^t \\ U_g \end{bmatrix} = \begin{bmatrix} 0 \\ P_g \end{bmatrix} \quad (2)$$

where U^t and U_g are the absolute displacement vector of the superstructure and the ground displacement vector enforced at the supports, respectively; M_g , C_g , and K_g are the mass, damping, and elastic-coupling matrices expressing the forces developed in the active degrees of freedom by the motion of the supports. M_{gg} , C_{gg} , and K_{gg} are the mass, damping, and stiffness matrices of the supports, respectively.

Finite element model of the bridge

A three-dimensional finite-element model of the bridge was constructed using SAP2000 software [48] (see Fig. 4). The model includes four types of elements. These are frame, shell, cable, and link elements. Frame elements were used to model the towers of the bridge. Four node shell elements were used to model the bridge deck and the main pyramidal piers. Each node of the shell or the frame elements has six degrees of freedom. These are translations in X , Y , and Z directions and rotations about these directions.

The material nonlinearity of cables was taken into account by modeling them to carry tension only. Therefore, if subjected to compression, their stiffness will be taken equal to zero (see Fig. 5). The cables' geometric nonlinearity was considered using the modified models of elasticity method suggested by Ernst [49] using the following equation:

$$E_{mod} = \frac{E_{ori}}{1 + \frac{(WL)^2 (EA)_{ori}}{12T_0^3}} \quad (3)$$

where E_{mod} is the modified modulus of elasticity of cables, E_{ori} is the original cable modulus of elasticity, W is the weight per unit length of the cable, L is the horizontal projected length of the cable, $(EA)_{ori}$ is the cable original axial stiffness, and T_0 is the tension force in the cable.

Due to the lack of information about the specific details and composition of the elastomeric bearings, they were designed as lead-rubber bearings with the general behavior shown in Fig. 5 [50]. Moreover, the design was checked to match the general behavior of full-scale experimental tests [51]. The main properties of the designed bearings in the

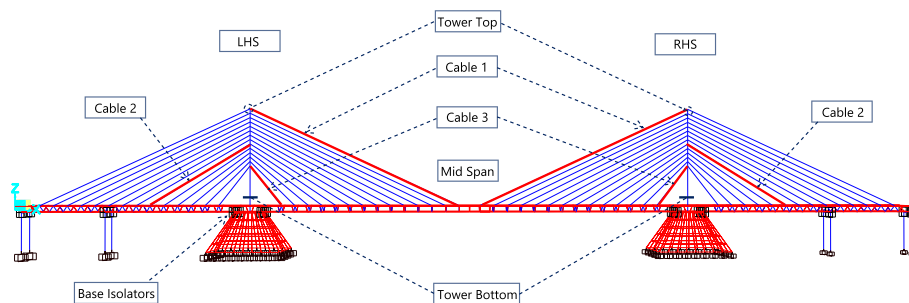


Fig. 4 Three-dimensional model of the bridge

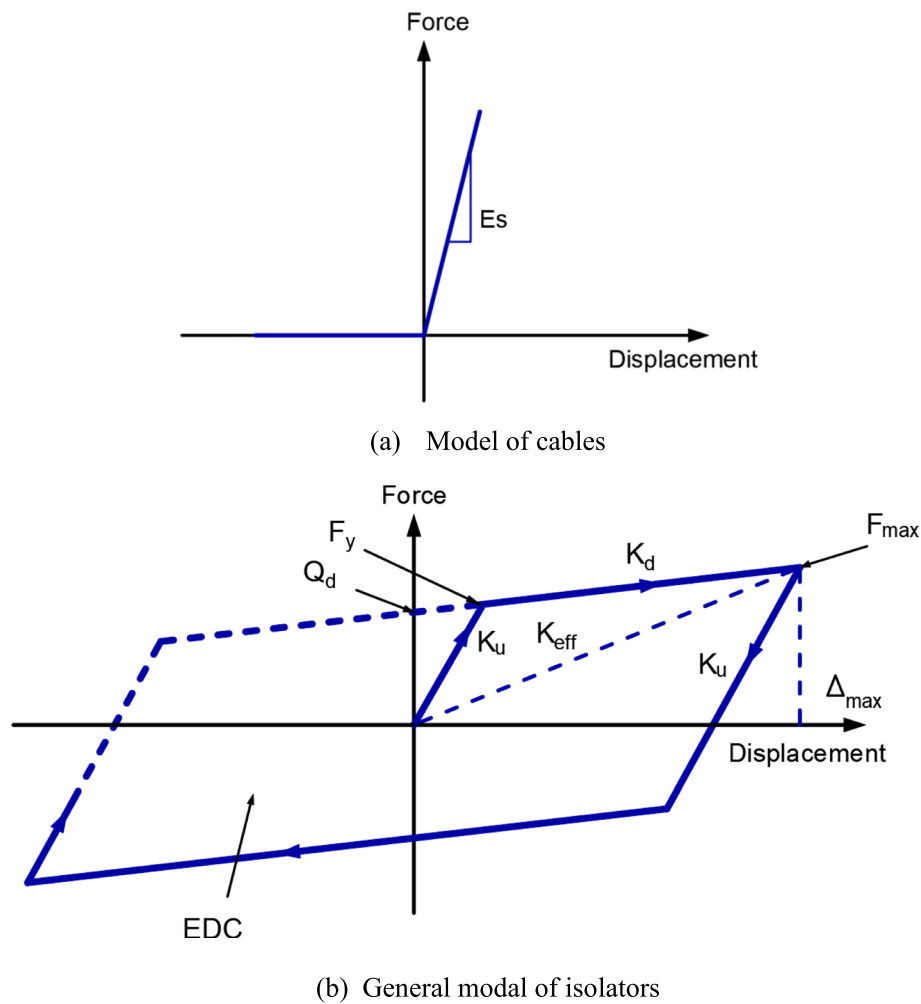


Fig. 5 Utilized model for cables and isolation bearings. **a** Model of cables. **b** General modal of isolators

horizontal direction are $K_u=157$ kN/mm, $K_{eff} = 24.3$ kN/mm, $K_d=15.7$ kN/mm, and $F_y=863$ kN. In the vertical direction, however, the bearings were assumed to be rigid. The bearings were modeled utilizing the nonlinear dissipative Wen model link elements in order to represent the dynamic behavior of the isolators under seismic action. These link elements were located between the top of the piers and the bottom of the deck. Due to the large size of the raft under the pier in addition to the large number of piles underneath, the bridge was assumed to be fixed at the foundation level (see Fig. 3).

Modeling of multi-support excitation

Multi-Support Excitation occurs due to the phenomenon of spatial variation of earthquake ground motion. It can be attributed to three mechanisms as following [33, 52]:

- 1) "Wave passage effect" which occurs due to difference in arrival times of seismic waves at different supports. The apparent wave propagation velocity mainly controls this effect.

- 2) "Incoherence effect" which means loss of coherence of the seismic waves. It results from multiple reflection and refraction of the seismic waves during their propagation through highly inhomogeneous soil medium.
- 3) "Local soil effect" where the amplitude and the frequency content of the seismic wave changes according to local soil conditions.

In the current study, the spatial variability was represented in terms of the wave passage effect which was simulated via different delay times between the arrival of the ground motion to the left supports and their arrival to the right ones. Based on the general types of soils located in Egypt, this delay time was estimated to range between 0 and 3 s for the specific length of Aswan cable-stayed bridge. Therefore, different delay times of 0, 1, 2, and 3 s were considered in the current analysis.

Five earthquakes were utilized in the current study. They were selected to represent a variety of earthquakes that might occur in Egypt. The main data of the utilized earthquakes are listed in Table 4. Moreover, the displacement and acceleration time histories of these earthquakes are shown in Fig. 6. Furthermore, the acceleration and displacement response spectra for these earthquakes are plotted in Fig. 7.

Results and discussion

The vibration properties of the bridge are summarized in Table 5. The participating mass ratios in different directions along with the description of each mode are given in the table. Moreover, the shapes of these modes are illustrated in Fig. 8.

The bridge was analyzed under different earthquakes acting in its longitudinal direction. Different wave propagation delay times between the excitations at the supports were considered to represent spatial non-synchronous seismic excitations. The delay times considered include zero delay representing the case of synchronous excitations and 1-, 2-, and 3-s delay representing different velocities of the seismic excitation (i.e., different soil conditions). The effect of such delay on key response parameters of the bridge was evaluated. These key response parameters include the total base shear of the bridge, the shear forces acting on the towers, longitudinal top displacement of the towers, forces in selected cables, vertical deflection at mid span of the bridge, and force displacement hysteric behavior of the seismic isolators. Table 6 summarizes the maximum results of these key responses obtained from different analyzed cases. The table also summarizes the average results obtained due to different earthquakes.

Table 4 Utilized earthquake data

E.Q.	Year	Station	Mechanism	Magnitude	PGA %g	PGV cm/s	Vs30 (m/s)
Imperial Valley	1979	Cerro Prieto CP, USA	Strike Slip	6.53	16.66	19.09	471.53
Loma Prieta	1989	Andeson Dam (Labut), USA	Reverse Oblique	6.93	25.15	22.34	488.77
San Fernando	1971	Castaic-Old Ridge Route, USA	Reverse	6.61	44.39	33.27	450.28
Tabas	1978	Kashmar, Iran	Reverse	7.35	3.83	7.76	280.26
Bam	2003	Ravar, Iran	Strike Slip	6.6	1.29	1.71	280.26

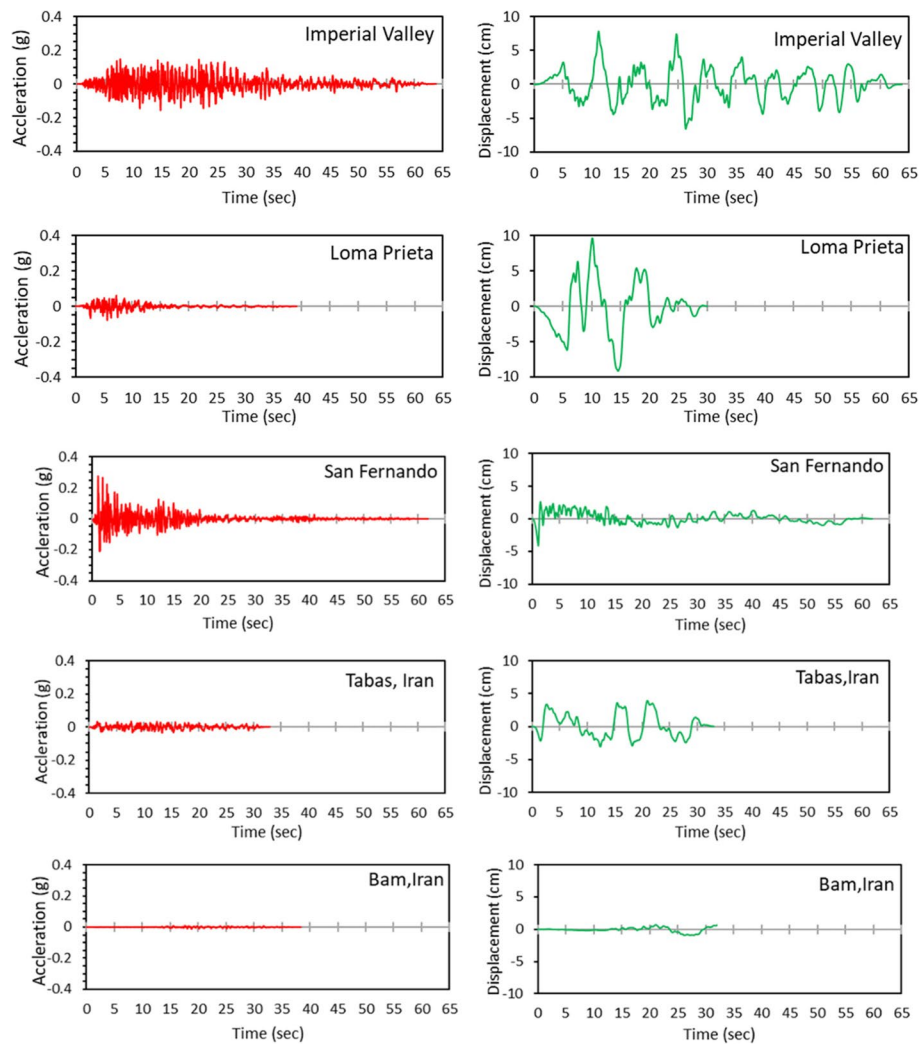
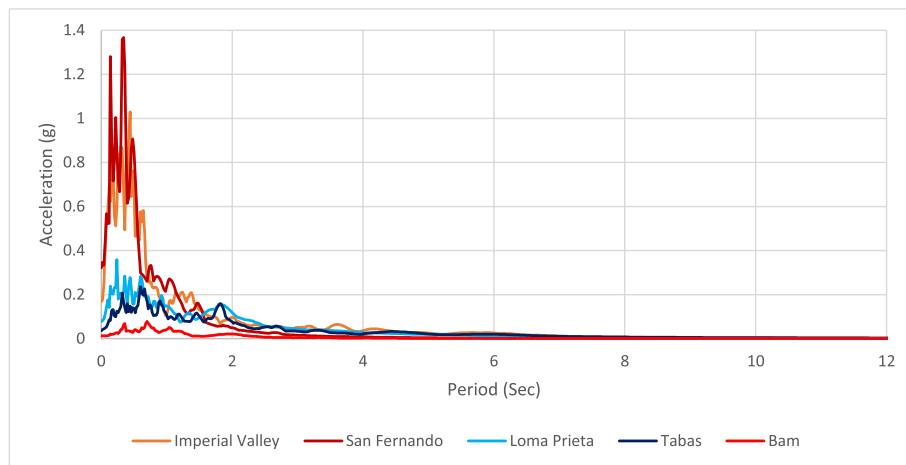
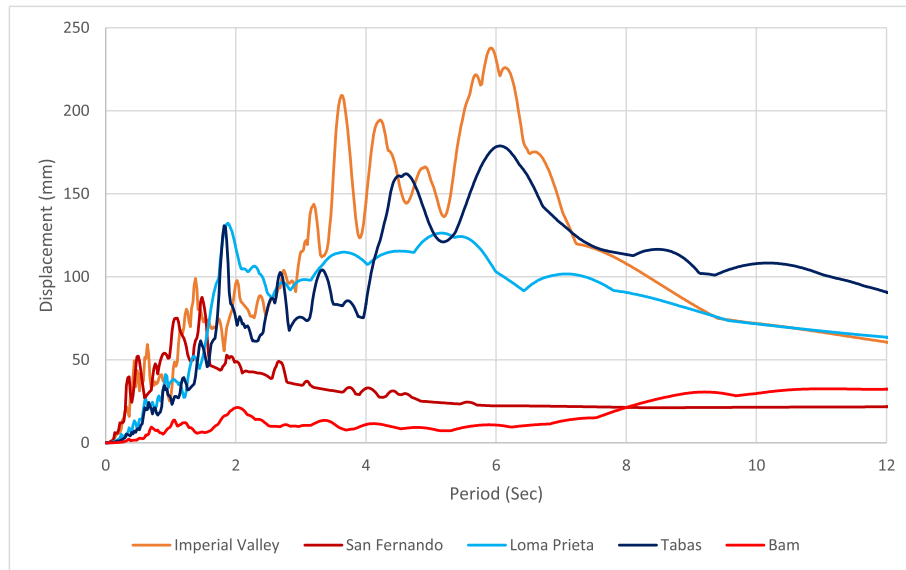


Fig. 6 Acceleration and displacement time history of the utilized earthquakes

Figure 9 shows the variation of the base shear overweight for different delay times under different earthquakes. The figure also shows the average values of the base shear overweight. It is observed that the highest base shear occurs under Imperial Valley earthquake and the lowest one occurs under Bam earthquake. Moreover, while the average base shear overweight ratio was 4.98% in case of synchronous excitations, it reached 3.83%, 3.91%, and 3.37% for delay times of 1, 2, and 3 s, respectively. Generally speaking, increasing the delay time causes a moderate reduction in the base shear response. This favorable behavior can be attributed to the fact that when the earthquake hits all support simultaneously the peak seismic inertia forces affects the whole bridge leading to high values of base shear. On the other hand, when there is delay between the arrivals of the seismic excitation, the peak effect becomes non-synchronous causing a moderate reduction of the base shear response. Moreover, existence of seismic isolators accommodates the different displacements at the bridge supports due to non-synchronous excitations. This observation is compatible with Tzanetos et al. [53] who stated that “seismic isolation of long span bridges generally reduces or eliminates the effects of non-synchronous



(a) Acceleration response spectra



(b) Displacement response spectra

Fig. 7 Response spectra of utilized earthquakes. **a** Acceleration response spectra. **b** Displacement response spectra

input motion". This might not be the case if the bridge is rigidly attached to its supporting system. In the latter case, non-synchronous excitations may cause an increase of the forces acting on the bridge.

The maximum shear forces acting at the bottom section of the left and the right towers are shown in Fig. 10, and the corresponding average values for both towers are shown in Fig. 11. The highest shear forces occur under Imperial Valley earthquake, and the lowest ones occur under Bam earthquake. Moreover, the shear forces in both towers exhibit general reduction for different delay times with no specific trend. It is worth mentioning that, from a design point of view, the maximum shear force under Imperial Valley earthquake reaches 3349 kN which is far less than the elastic capacity of the tower.

Figure 12 shows the towers top longitudinal displacement under different earthquakes, and Fig. 13 shows the average response for all used earthquakes. Again, the Imperial

Table 5 Modal properties

Mode no.	Period (sec)	Modal participating mass ratios (%)						Description
		Longitudinal direction	Longitudinal direction (cumulative)	Lateral direction	Lateral direction (cumulative)	Vertical direction	Vertical direction (cumulative)	
1	11.86	0	0	42.73	42.73	0	0	Out of plane bending of pylons (first mode—in phase)
2	11.62	0	0	0	42.73	0	0	Out of plane bending of pylons (first mode—out of phase)
3	6.14	89.52	89.52	0	42.73	0	0	Longitudinal vibration through seismic isolation interface
4	5.34	0	89.52	0	42.73	0	0	transverse vibration through seismic isolation interface (out of phase)
5	5.12	0	89.52	8.44	51.17	0	0	Transverse bending of deck (first mode)
6	4.72	0	89.52	38.19	89.36	0	0	Transverse vibration through seismic isolation interface (in phase)
7	1.69	0	89.52	0	89.36	0	0	Transverse bending of deck (second mode) accompanied with transverse vibration through seismic isolation interface (out of phase)
8	1.65	0	89.52	0	89.36	27.2	27.2	Vertical bending of main span deck (first mode)
9	1.18	0	89.52	0.03	89.39	0	27.2	Out of plane bending of pylons (second mode—in phase)
10	1.1	0	89.53	0	89.39	0	27.2	Vertical bending of main span deck (second mode)

Valley earthquake causes the highest displacements and Bam earthquake gives the lowest ones. Also, the general trend of the tower displacement is to decrease with the increase of the delay time. Reductions in the displacements ranges between 30 and 45% in case of non-synchronous excitations compared to synchronous excitations. A sample

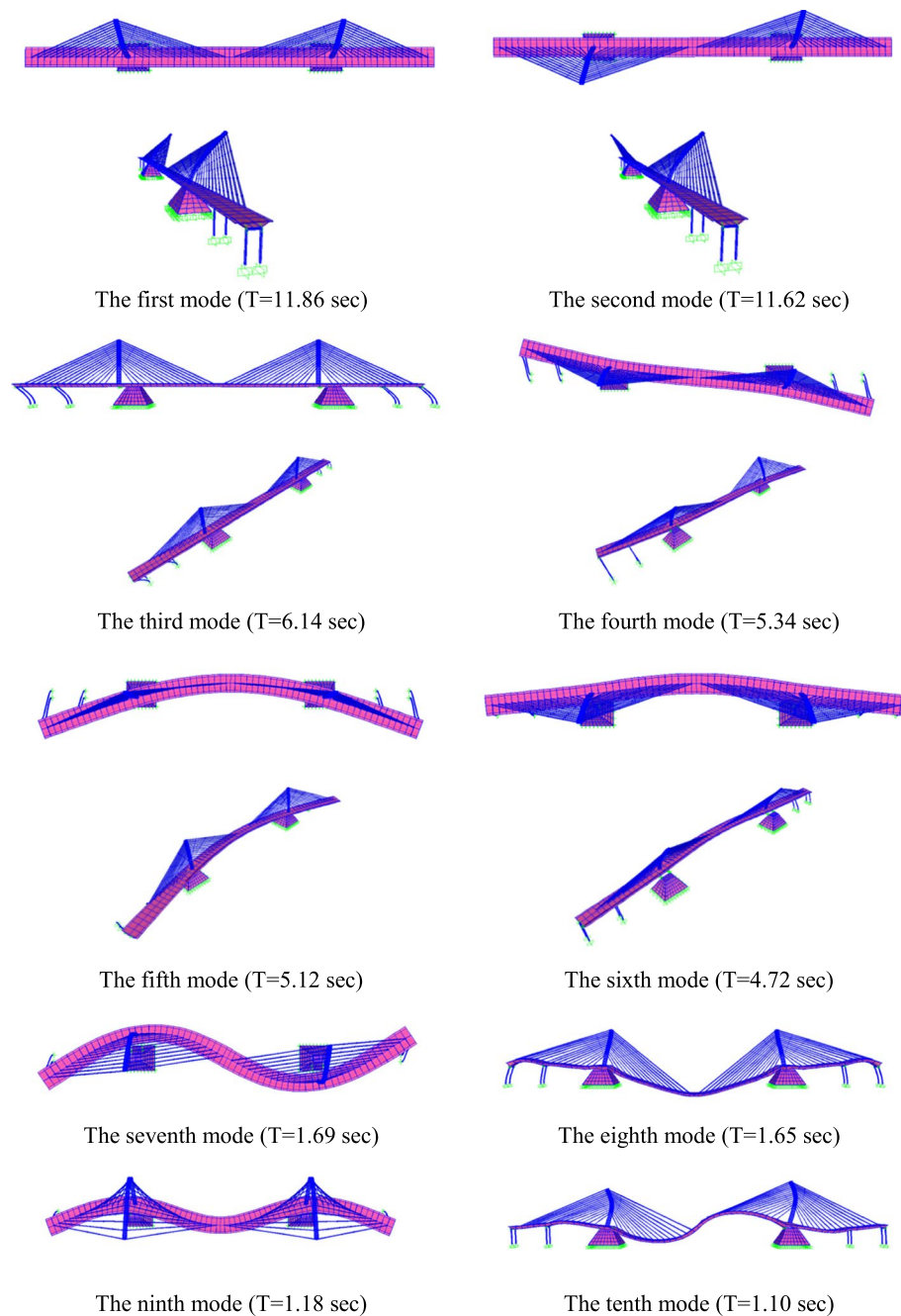


Fig. 8 Analytical modes of vibration of the bridge

of the displacement time history at the top of the left tower is shown in Fig. 14. Obviously, the maximum displacements occur for the no delay case.

Figure 15 shows the variation of resulting cable forces for three selected cables (refer to Fig. 4), and Fig. 16 shows the average values of forces in these cables for different earthquakes. Moreover, Fig. 17 shows the time history of force resulting in cable No. 1 at the right-hand side of the bridge for different delay times. It can be observed that the maximum response in all cables under all earthquakes occurs in the

Table 6 Maximum responses of the bridge under different excitations and delay times

Excitation	Delay (s)	Pylon top displacement (cm)		Shear at the bottom of the pylon (kN)		Cable force (kN)						Base isolator		Vertical Displacement at midspan (cm)	Base shear/weight (%)
						Cable 1		Cable 2		Cable 3		Displacement (cm)	Force (kN)		
		Left	Right	Left	Right	Left	Right	Left	Right						
ImperialVally	0	13.4	11.5	3349	3234	14044	10686	14044	10686	11446	10686	9.46	1359	8.65	10.00
	1	7.9	7.3	2054	2385	9010	8724	5153	4567	8030	8089	10.95	1449	5.62	8.59
	2	6.9	7.7	2347	2399	7675	8035	7675	5081	7571	6979	7.40	1235	4.67	8.15
	3	5.9	7.6	2365	2096	8581	9681	6589	7205	8635	7698	8.45	1289	6.11	8.48
San Fernando	0	5.2	3.9	2165	2232	8124	8407	6948	5553	7862	6841	5.87	1144	5.56	7.88
	1	2.8	2.8	1580	1539	5081	6508	3770	3937	6622	5887	3.81	1020	5.27	6.20
	2	3.2	3.7	1912	2513	7461	8721	5484	5778	7856	6925	3.70	1018	6.28	6.26
	3	2.1	1.9	2125	1920	6122	6189	4326	3754	3573	8588	3.79	1018	4.03	3.82
Loma Prieta	0	9.4	8.1	3037	2355	10560	12820	5694	4846	6319	8354	5.90	1142	7.60	4.16
	1	7.1	5.5	1911	1048	4824	5774	2148	2210	3050	3863	6.47	1180	3.81	2.63
	2	3.4	4.5	2002	2204	8260	8295	5566	4154	9539	6498	4.53	1051	6.31	3.00
	3	4.9	5.2	1840	1644	9078	7674	5119	5538	4231	6463	3.98	1001	4.40	2.41
Tabas	0	7.5	6.9	2585	2531	9453	8961	4328	4256	9704	9420	5.33	1111	6.95	2.00
	1	5.0	4.8	1075	1264	5412	5416	3198	2579	5224	3773	4.20	1041	3.57	1.44
	2	5.0	3.4	2402	2296	8467	6348	4747	4161	1080	5363	6.20	1163	7.24	1.72
	3	6.5	5.2	1693	1675	9390	5985	4958	3447	6245	5256	5.69	1132	4.90	1.63
Bam	0	2.2	2.6	767	779	3456	2894	2316	1238	1951	2489	0.74	426	2.61	0.84
	1	1.3	1.7	266	374	1504	1234	841	887	590	552	0.83	474	1.04	0.31
	2	1.2	1.8	268	356	2110	1294	894	923	965	894	0.90	461	1.12	0.42
	3	1.2	1.7	299	343	2530	1359	925	819	1074	1310	0.98	507	1.49	0.51
Average Values	0	7.5	6.6	2380	2226	9127	8754	6666	5316	7456	7558	5.46	1036	6.27	4.98
	1	4.8	4.4	1377	1322	5166	5531	3022	2836	4703	4433	5.25	1033	3.86	3.83
	2	3.9	4.2	1786	1954	6795	6539	4873	4019	5402	5332	4.55	986	5.13	3.91
	3	4.1	4.3	1664	1536	7140	6178	4383	4153	4752	5863	4.58	989	4.19	3.37

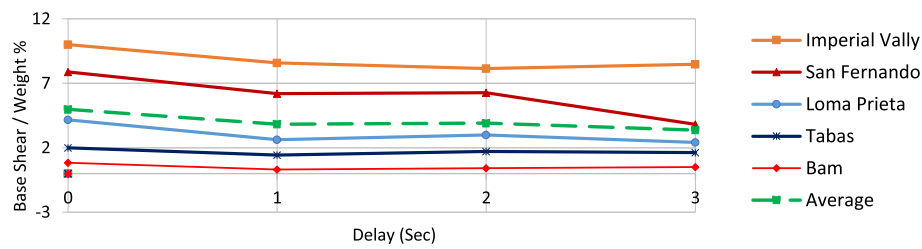


Fig. 9 Base shear/weight for different earthquakes

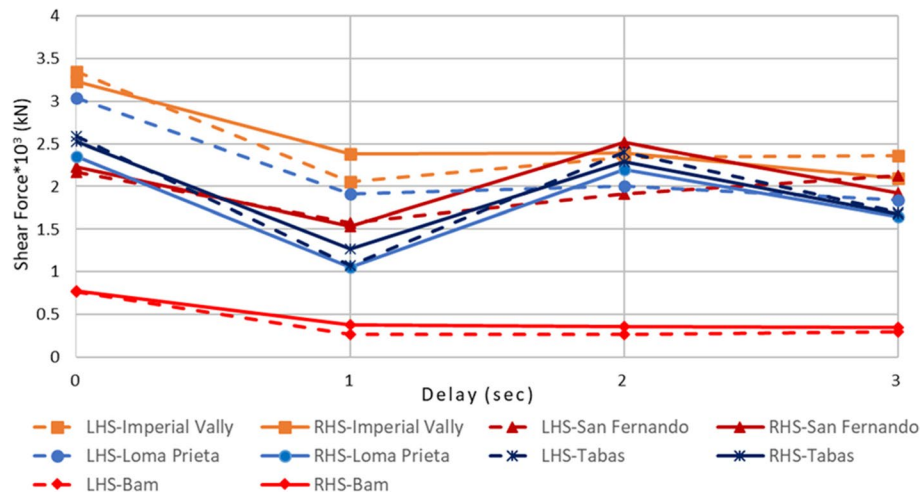


Fig. 10 Maximum shear force at tower bottom under different earthquakes



Fig. 11 Average shear force at tower bottom

synchronous excitations, and the general trend of the cable forces is to decrease with the delay time with some fluctuations.

Figure 18 shows the maximum deflection at mid span of the bridge. The figure also shows the average values under different excitations. It is obvious that the deflections generally decrease with the increase in the delay time with no specific trend.

Figure 19 shows the lateral force displacement loops for a selected base isolator located at the left pier and the corresponding one located at the right pier. For synchronous excitation, the behavior of the two isolators is nearly identical. However, for non-synchronous excitation, the behavior of the two isolators is quite different. Enlarged force displacement loops may take place at the left isolators or at the right

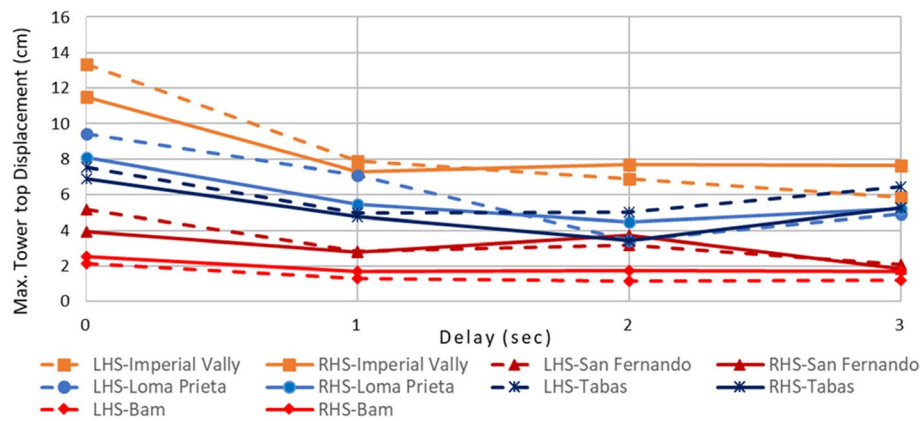


Fig. 12 Maximum tower top displacement under different earthquakes

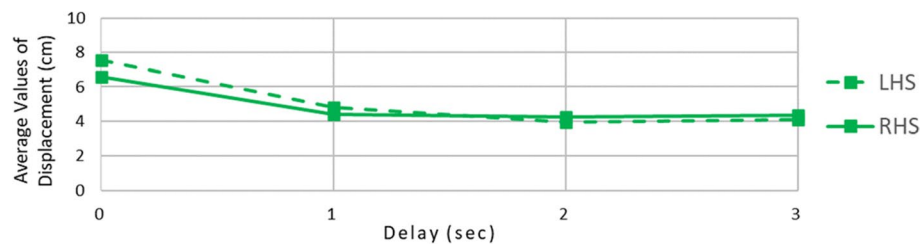


Fig. 13 Average tower top displacement

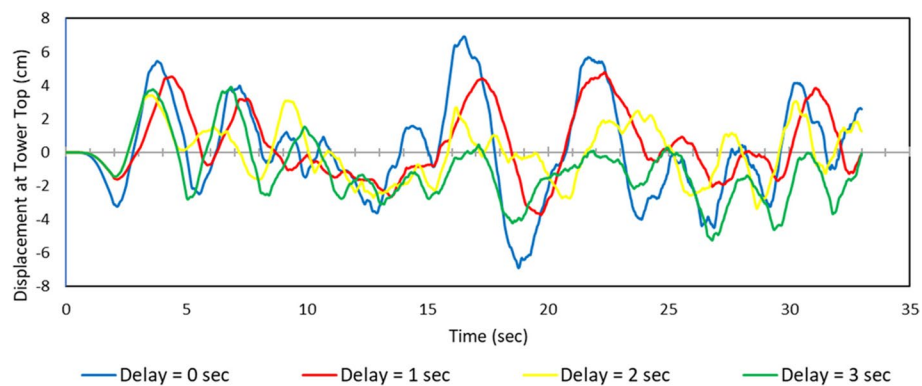


Fig. 14 Time history of displacement of LHS-tower top point under Tabas earthquake

ones depending on the earthquake excitation delay time. In all cases, considerable energy is favorably dissipated in the isolators.

Results presented in Figs. 9, 10, 11, 12, 13, 14, 15, 16, 17, 18 and 19 and in Table 6 suggest that when the effect of the time delay of ground motions is considered, the supports of such long span bridge will motion in different phases, which consequently result in the cancellation of inertia forces, and hence, the reduction of the overall bridge response. Such results are in agreement with the results in the studies carried out by Sextos et al. [35], Mylonakis et al. [54], and Zang et al. [55]. This is attributed to the flexibility of the bridge structural system and/or existence of seismic isolation

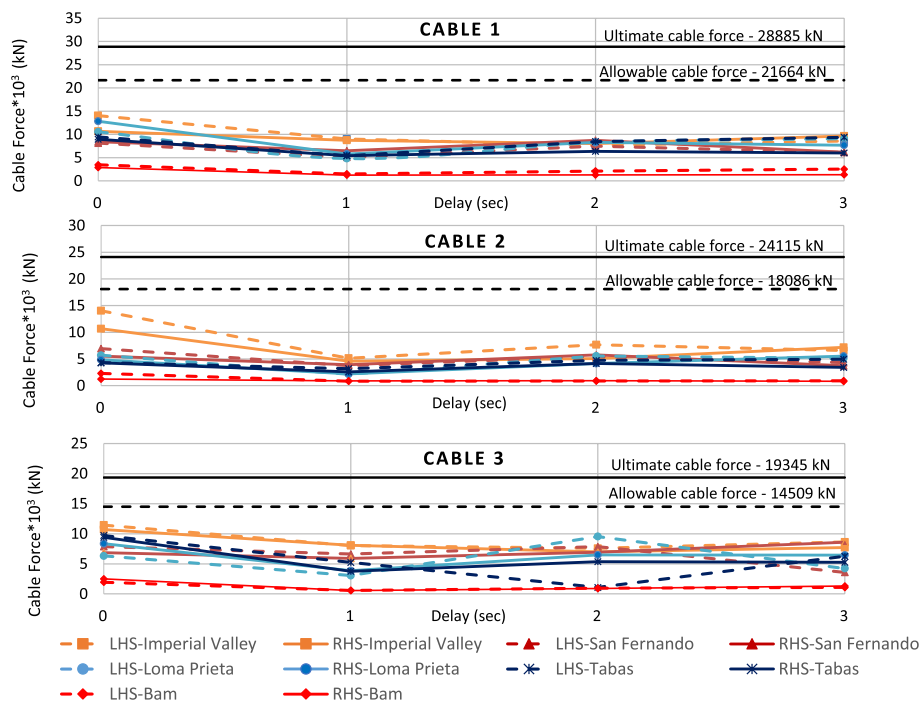


Fig. 15 Maximum force in cables under different earthquakes

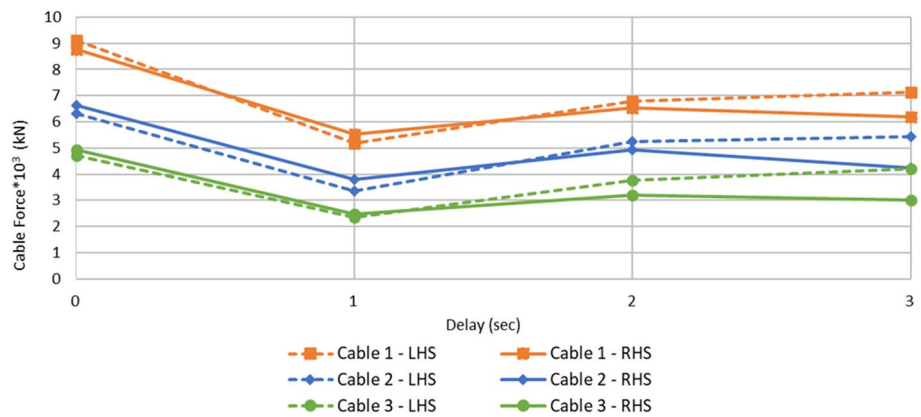


Fig. 16 Average force in cables

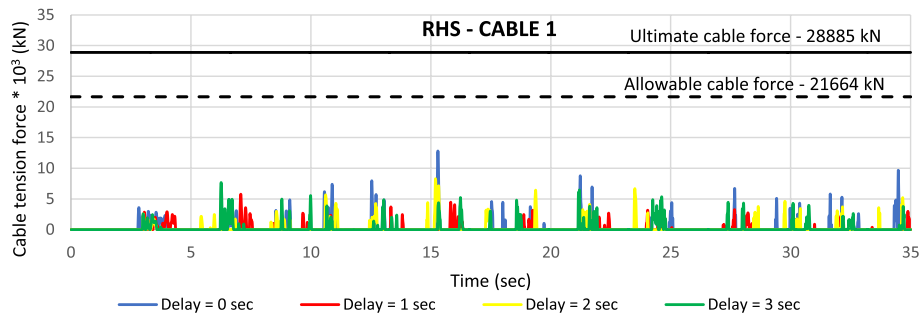


Fig. 17 Time history of forces in cables

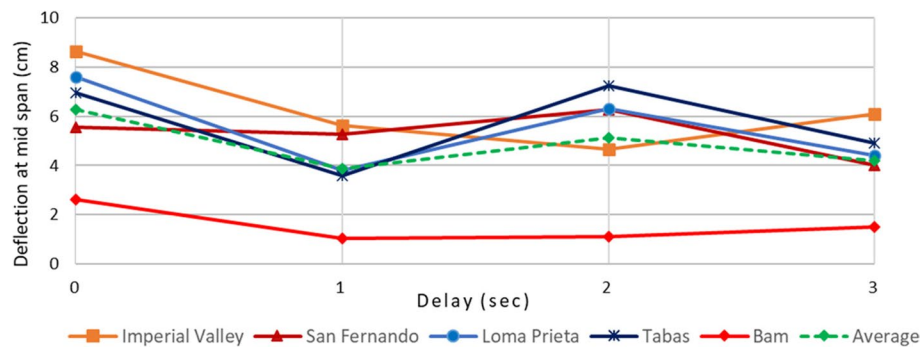


Fig. 18 Maximum deflection at mid span

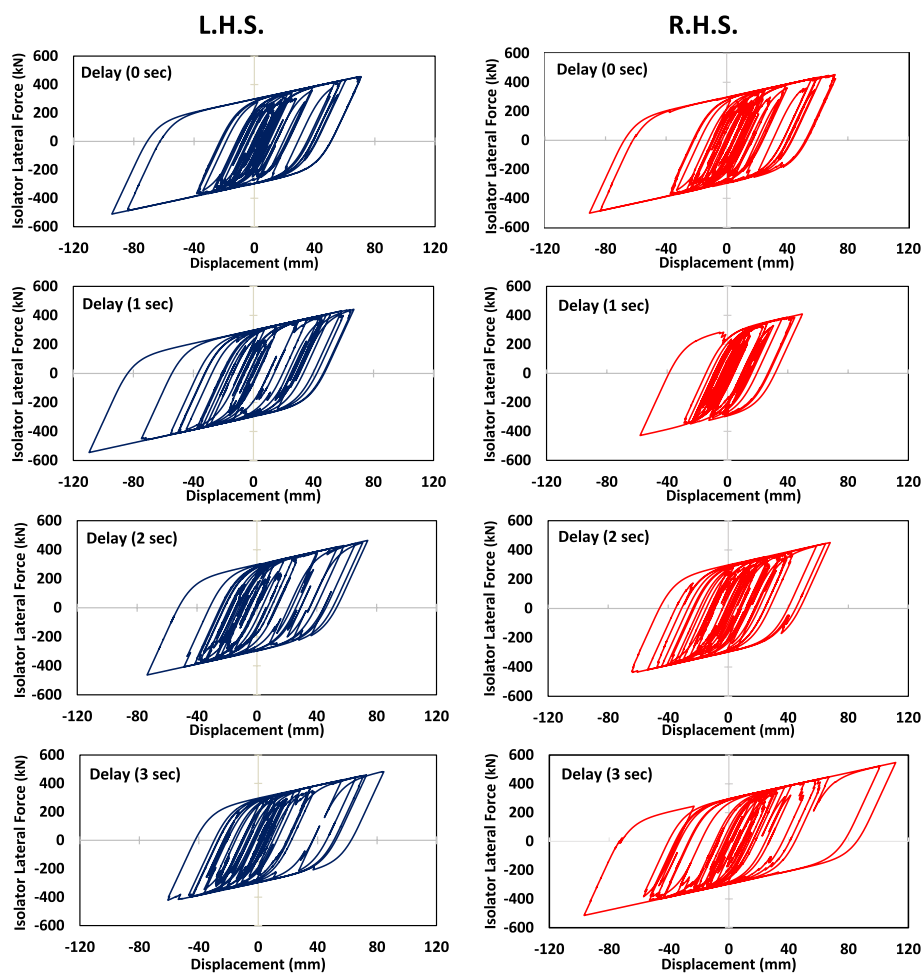


Fig. 19 Force-displacement loop of base isolator under Imperial Valley earthquake

in these studies. On the other hand, the current results are in contradiction with the results of Leger et al. [56] and Bayrak [57]. The main reason might be attributed to the rigid attachment of the relatively stiff columns to the girder in these studies. Consequently, it can be concluded that the flexibility of the overall bridge (provided by the

flexibility of the bridge structural system itself and/or by existence of seismic isolation) might have a favorable effect in case of non-synchronous earthquake ground motion excitations.

Conclusions

From the results of the current study, the following conclusions can be drawn:

1. Spatial variability of earthquake ground motion has, in general, a favorable effect on most of the studied bridge response parameters. For example, while the average base shear over weight ratio was 4.98% in case of synchronous excitations, it reached 3.83%, 3.91%, and 3.37% for delay times of 1, 2, and 3 s, respectively. Moreover, the general trend of the tower displacement was to decrease with the increase of the delay time. Reductions in the displacements ranged between 30 and 45% in case of non-synchronous excitations compared to synchronous excitations.
2. This favorable behavior can be attributed to the fact that when the earthquake hits all supports simultaneously, the peak seismic inertia forces affect the whole bridge leading to high response values. On the other hand, when the effect of the time delay of ground motions is considered, the supports of such long span bridge will motion in different phases, resulting in the cancellation of inertia forces and hence, the reduction of the overall bridge responses.
3. The existence of seismic isolators accommodates the different displacements at the bridge supports due to non-synchronous excitations. This might not be the case if the bridge is rigidly attached to its supporting system. In the latter case, non-synchronous excitations may cause an increase of the forces acting on the bridge.
4. The flexibility of the overall bridge (provided by the flexibility of the bridge structural system and/or by existence of seismic isolation) might have a favorable effect in case of non-synchronous earthquake ground motion excitations.
5. It should be mentioned that the above conclusions are limited to this specific bridge and similar ones. But they cannot be generalized to bridges having other configurations. It might be stated that the effect of non-synchronous earthquake excitations on the response of a bridge is complex and depends on the soil condition, the characteristics of the earthquake excitations, and the specific structural system of the bridge.

Abbreviations

ISE	Identical support excitation
MSE	Multi-support excitation
TFPS	Triple Friction Pendulum System
PGA	Peak ground acceleration
PGV	Peak ground velocity

Acknowledgements

Not applicable.

Authors' contributions

MS analyzed the bridge, contributed to the preparation of the figures, and interpreted the results. MH, MA, EH, and MG collected the data, participated in the analysis, and contributed to the preparation of the figures. AS interpreted the

results and contributed to writing the manuscript. AE was a major contributor in analyzing the data and writing the manuscript. The authors read and approved the final manuscript.

Funding

Not applicable.

Availability of data and materials

Not applicable.

Declarations

Competing interests

The authors declare that they have no competing interests.

Received: 13 April 2022 Accepted: 23 July 2022

Published online: 17 August 2022

References

1. Ali H-EM, Abdel-Ghaffar AM (1995) Seismic Passive Control of Cable-Stayed Bridges. *Shock and Vibration* 2:918721. <https://doi.org/10.3233/SAV-1995-2401>
2. Abdel Raheem S, Hayashikawa T (2003) Parametric study on steel tower seismic response of cable-stayed bridges under great earthquake ground motion. *Struct Eng Earthq Eng* 20:25–41
3. Talebinejad I, Fischer C, Ansari F (2011) Numerical evaluation of vibration-based methods for damage assessment of cable-stayed bridges. *Comput Aided Civil Infrastruct Eng* 26(3):239–251
4. Cucuzza R, Costi C, Rosso MM, Domaneschi M, Marano GC, Masera D (2022) Optimal strengthening by steel truss arches in prestressed girder bridges. *Bridg Eng* 1478–4637
5. Clemente P, Bongiovanni G, Buffarini G, Saitta F (2019) Structural health status assessment of a cable-stayed bridge by means of experimental vibration analysis. *J Civ Struct Heal Monit* 9(5):655–669
6. Hao Q, Jufeng S, Pingming H (2017) Study on dynamic characteristics and seismic response of the extradosed cable-stayed bridge with single pylon and single cable plane. *J Civ Struct Heal Monit* 7(5):589–599
7. Elkady AZ, Seleemah MA, Ansari F (2018) Structural response of a cable-stayed bridge subjected to lateral seismic excitations. *J Civ Struct Heal Monit* 8(3):417–430
8. Javanmardi A, Ibrahim Z, Ghaedi K, Khatibi H (2017) Seismic response characteristics of a base isolated cable-stayed bridge under moderate and strong ground motions. *Arch Civil Mech Eng* 17:419–432
9. Camara A, Astiz MA (2014) Analysis and control of cable-stayed bridges subject to seismic action. *Struct Eng Int* 24(1):27–36
10. Zhang N, Xia H, De Roeck G (2010) Dynamic analysis of a train-bridge system under multi-support seismic excitations. *J Mech Sci Technol* 24(11):2181–2188
11. Liu W, Xu X, Wang R, Wang Z, Wu X (2006) Vibration reduction design of the Hangzhou Bay cable-stayed bridges. *Structural Engineering and Mechanics* 24:339–354. <https://doi.org/10.12989/sem.2006.24.3.339>
12. Camara A, Astiz MA (2012) Pushover analysis for the seismic response prediction of cable-stayed bridges under multi-directional excitation. *Eng Struct* 41:444–455
13. El Ouni MH, Ben KN, Preumont A (2012) Numerical and experimental dynamic analysis and control of a cable stayed bridge under parametric excitation. *Eng Struct* 45:244–256
14. Zanardo G, Hao H, Modena C (2002) Seismic response of multi-span simply supported bridges to a spatially varying earthquake ground motion. *Earthq Eng Struct Dyn* 31(6):1325–1345
15. Lin JH, Zhang YH, Li QS, Williams FW (2004) Seismic spatial effects for long-span bridges, using the pseudo excitation method. *Eng Struct* 26(9):1207–1216
16. Bi K, Hao H, Chouw N (2011) Influence of ground motion spatial variation, site condition and SSI on the required separation distances of bridge structures to avoid seismic pounding. *Earthq Eng Struct Dyn* 40(9):1027–1043
17. Mehanny SSF, Ramadan OMO, El Howary HA (2014) Assessment of bridge vulnerability due to seismic excitations considering wave passage effects. *Eng Struct* 70:197–207
18. Alexander NA (2008) Multi-support excitation of single span bridges, using real seismic ground motion recorded at the SMART-1 array. *Comput Struct* 86(1):88–103
19. Shehata EAR, Toshiro H (2007) Seismic protection of cable-stayed bridges under multiple-support excitations, 4th International Conference on Earthquake Geotechnical Engineering, June Volume: 4
20. Tonyali Z, Ates S, Adanur S (2019) Spatially variable effects on seismic response of the cable-stayed bridges considering local soil site conditions. *Struct Eng Mech* 70(2):143–152
21. Ates S, Atmaca B, Yildirim E, Demiroz NA (2013) Effects of soil-structure interaction on construction stage analysis of highway bridges. *Computers and Concrete* 12:169–186. <https://doi.org/10.12989/cac.2013.12.2.169>
22. Ateş Ş, Tonyali Z, Soyuluk K, Semberou AMS (2018) Effectiveness of Soil–Structure Interaction and Dynamic Characteristics on Cable-Stayed Bridges Subjected to Multiple Support Excitation. *International Journal of Steel Structures* 18:554–568. <https://doi.org/10.1007/s13296-018-0069-z>
23. Cucuzza R, Rosso MM, Aloisio A, Melchiorre J, Giudice ML, Marano GC (2022) Size and shape optimization of a guyed mast structure under wind, ice and seismic loading. *Appl Sci* 12(10):4875–4832
24. Kiureghian AD, Neuenhofer A (1992) Response spectrum method for multi-support seismic excitations. *Earthq Eng Struct Dyn* 21(8):713–740

25. Heredia Zavoni E, Vanmarcke Erik H (1994) Seismic random vibration analysis of multisupport structural systems. *J Eng Mech* 120(5):1107–1128
26. Dumanoglu AA, Soylik K (2003) A stochastic analysis of long span structures subjected to spatially varying ground motions including the site-response effect. *Eng Struct* 25(10):1301–1310
27. Hao H (1998) A parametric study of the required seating length for bridge decks during earthquake. *Earthq Eng Struct Dyn* 27(1):91–103
28. Somerville PG, McLaren JP, Sen MK, Helmberger DV (1991) The influence of site conditions on the spatial incoherence of ground motions. *Struct Saf* 10(1):1–13
29. Vanmarcke EH, Fenton GA (1991) Conditioned simulation of local fields of earthquake ground motion. *Struct Saf* 10(1):247–264
30. Bi K, Hao H (2012) Modelling and simulation of spatially varying earthquake ground motions at sites with varying conditions. *Probabilistic Eng Mech* 29:92–104
31. Liao S, Zerva A (2006) Physically compliant, conditionally simulated spatially variable seismic ground motions for performance-based design. *Earthq Eng Struct Dyn* 35(7):891–919
32. Konakli K, Der Kiureghian A (2012) Simulation of spatially varying ground motions including incoherence, wave-passage and differential site-response effects. *Earthq Eng Struct Dyn* 41(3):495–513
33. Saxena V, Deodatis G, Shinozuka M (2000) Effect of spatial variation of earthquake ground motion on the nonlinear dynamic response of highway bridges. In: *Proceedings of 12th World Conference on Earthquake Engineering*. Auckland, New Zealand
34. Deodatis G (1996) Non-stationary stochastic vector processes: seismic ground motion applications. *Probabilistic Eng Mech* 11(3):149–167
35. Sextos A, Karakostas C, Lekidis V, Papadopoulos S (2015) Multiple support seismic excitation of the Evripos bridge based on free-field and on-structure recordings. *Struct Infrastruct Eng* 11(11):1510–1523
36. Fontara I-KM, Titirla MD, Wuttke F, Athanatopoulou AM, Manolis GD, Sextos AG (2015) Multiple support excitation of a bridge based on beam analysis of the subsoil-structure-interaction phenomenon. In: *5th ECCOMAS Thematic Conference on Computational Methods in Structural Dynamics and Earthquake Engineering*. Crete Island, Greece
37. Ramadan OMO, Mehanny SSF, Elhowary HA (2015) Seismic vulnerability of box girder continuous bridges under spatially variable ground motions. *Bull Earthq Eng* 13(6):1727–1748
38. Zhong J, Jeon J-S, Yuan W, DesRoches R (2017) Impact of spatial variability parameters on seismic fragilities of a cable-stayed bridge subjected to differential support motions. *J Bridg Eng* 22(6):04017013
39. Atmaca B, Yurdakul M, Ateş S (2014) Nonlinear dynamic analysis of base isolated cable-stayed bridge under earthquake excitations. *Soil Dyn Earthq Eng* 66:314–318
40. Abdel Zaher A, Rabei M, El-Attar A, Kunieda M, Nakamura H (2006) Ambient vibration test of Aswan cable stayed bridge. *J Appl Mech* 9:85–93
41. Patel V ka., Panchal VR, Soni DP (2017) Effect of multi-support excitation on seismic behavior of TFPS-isolated cable stayed bridge. *International Journal of Advance Engineering and Research Development*
42. Masrilayanti, Riza A, Ruddy K, Zakpar S (2019) Behaviour of cable-stayed bridge's girder to multi-support excitation. In: *MATEC Web of Conferences*, vol 276, p 01037
43. Abou-Rayyan A (2014) Dynamic assessment of cable-stayed bridges in Egypt. *Int J Civil Eng* 3:67–74
44. Atmaca B (2021) Determination of proper post-tensioning cable force of cable-stayed footbridge with TLBO algorithm. *Steel Compos Struct* 40(6):805–816
45. Atmaca B, Dede T, Grzywinski M (2020) Optimization of cables size and prestressing force for a single pylon cable-stayed bridge with Jaya algorithm. *Steel Compos Struct* 34(6):853–862
46. Labib S, Bakhoum M (2000) Aswan Bridge Over The Nile. *Proceedings of the bridge engineering conference*. Sharm El-Sheik, Egypt, pp 601–608
47. General Authority for Roads, Bridges and Land Transport (GARBLT) Arab Republic of Egypt (2015) The Project for Improvement of the Bridge Management Capacity: project completion report. Japan International Cooperation Agency, Nippon Engineering Consultants Co., and Chodai Co.
48. SAP2000 Documentation (2012) Release 15.1.0. Computers and Structures, Inc., USA.
49. Ernst H (1965) Der E-Modul von Seilen unter Berücksichtigung. *Der Bauingenieur* 40(2):52–55
50. Constantinou MC, Soong TT, Dargush GF (1998) Passive energy dissipation systems for structural design and retrofit. *Multidisciplinary Center for Earthquake Engineering Research*
51. Constantinou MC, Whittaker AS, Kalpakidis Y, Fenz DM, Warn GP (2007) Performance of Seismic Isolation Hardware under Service and Seismic Loading. *Multidisciplinary Center for Earthquake Engineering Research MCEER*
52. Harichandran RS (1988) Local spatial variation of earthquake ground motion. In: Von Thun JL (ed) *Earthquake Engineering and Soil Dynamics II - Recent Advances in Ground-Motion Evaluation*. American Society of Civil Engineers, New York, pp 203–217
53. Tzanetos N, Elnashai AS, Hamdan FH, Antoniou S (2000) Inelastic dynamic response of RC bridges subjected to spatial non-synchronous earthquake motion. *Adv Struct Eng* 3(3):191–214
54. Mylonakis G, Papastamatiou D, Psycharis J, Mahmoud K (2001) Simplified Modeling of Bridge Response on Soft Soil to Nonuniform Seismic Excitation. *Journal of Bridge Engineering* 6:587–597. [https://doi.org/10.1061/\(ASCE\)1084-0702\(2001\)6:6\(587\)](https://doi.org/10.1061/(ASCE)1084-0702(2001)6:6(587))
55. Zhang T, Chen QJ, Chen ZH, Yang YS (2012) The Non-uniform Random Seismic Response Analysis of Long-span Bridge Structure Based on Pseudo-excitation Method. In: *15th World Conference on Earthquake Engineering*. Lisbon, Portugal
56. Leger P, Ide M, Paultre P (1990) Multiple-support seismic analysis of large structures. *Comput Struct* 36(6):1153–1158
57. Bayrak O (1996) Effect of multiple seismic input on the response of long multi-span bridge. In: *11th World Conference on Earthquake Engineering (WCEE)*

Publisher's Note

Springer Nature remains neutral with regard to jurisdictional claims in published maps and institutional affiliations.